C. R. Mecanique 338 (2010) 181–190

Contents lists available at ScienceDirect

Comptes Rendus Mecanique

www.sciencedirect.com

Combined effects of EDL and boundary slip on mean flow and its stability in microchannels

Xue-Yi You *, Lixiang Guo

School of Environmental Science and Engineering, Tianjin University, 300072 Tianjin, China

ARTICLE INFO

Article history:
Received 18 January 2010
Accepted after revision 31 March 2010
Available online 24 April 2010

Keywords:
Instability
Electrical double layer
Boundary slip
Flow stability
Microchannels

ABSTRACT

The effects of an electrical double layer (EDL), boundary slip and their combined effects on the microchannel flow stability are investigated. Instead of applying the traditional streaming electrical current balance (ECB) mode, a newly introduced electrical current density balance (ECDB) mode is used to compute the conduction current when the effects of EDL is considered. The modified N-S equations and Poisson–Boltzmann equation together with the ECDB mode and Navier slip boundary are the theoretical basis for the present approach. The stability analysis considering the modifications of EDL and boundary slip is built up by the small perturbation method. It is found that the effect of EDL results in inflexions on the mean velocity profile near walls and destabilizes the stability of flow. On the contrary, the effect of boundary slip stabilizes the stability of flow. The effectiveness of boundary slip on the mean velocity and flow stability is influenced strongly by the effect of EDL. The effect of boundary slip can be disappeared when the Zeta potential is large enough.

© 2010 Académie des sciences. Published by Elsevier Masson SAS. All rights reserved.

1. Introduction

In recent years, the sustained development of microfluidic devices and their potential applications in a variety of fields, particularly those associated with the so-called Micro-Electro-Mechanical-Systems (MEMS) have led to interests in the problem of fluid flow with hydraulic diameter ranging from 10^{-6} to 10^{-3} m called microflows [1–3]. Microfluidics dealing with the microflow has been receiving more and more attention in recent years. In many scientific and engineering applications, various innovative microfluidic systems are used to drive liquids and control flow stability [4,5]. Compared with the normal scale systems, one of the most important phenomena of microflows is the effects of the solid–liquid interface, which cannot be safely ignored. The effects of solid–liquid interface make the fundamental theories and regulations of microflows complex.

A large number of papers focusing on the liquid flows in microchannels have been reported over the recent decade. The researchers focus on two aspects: the flow characterization and flow stability analysis. The main microscale effects of microflow include apparent viscosity, boundary slip, electrical double layer (EDL), boundary roughness, etc. [6–12]. The laminar-to-turbulent transition of microflows has actually been studied by many researchers experimentally. Peng et al. [13] investigated the characteristics of water flow through rectangular ducts with hydraulic diameters ranging from 133 to 367 μm and the aspect ratios of 0.333 to 1. Their experiment results indicated that the flow transition occurred at Reynolds number of 200–700. Xu et al. [14] performed experiments of water in microchannels with hydraulic diameters ranging from 30 to 344 μm and the Reynolds numbers were 20 to 4000. Judy et al. [15] claimed that there was no transition to

* Corresponding author.
E-mail address: xyyou@tju.edu.cn (X.-Y. You).

1631-0721/$ – see front matter © 2010 Académie des sciences. Published by Elsevier Masson SAS. All rights reserved.
doi:10.1016/j.crme.2010.04.001

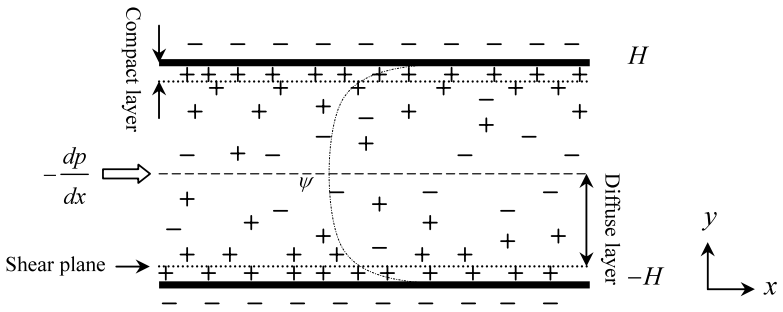

Fig. 1. The schematic illustration of the EDL compact and diffuse layer in microchannel.

turbulent flow when Re < 2000 in microtubes of fused silica and stainless steel. Sharp and Adrian [16] studied the laminar transition in liquid microtubes by PIV measurements, the system hydraulic diameters were 100–247 μm and the transition occurred at Reynolds number of 1800–2000. Hao et al. [17] used micro-PIV to investigate water flow in a trapezoidal silicon microchannel with hydraulic diameter 237 μm. The experimental results indicated the transition from laminar to turbulent flow occurred at the Reynolds number ranging in 1500–1800. Comparing the results of the above studies, it is found that the laboratory observations about laminar flow and laminar-to-turbulent transition are often inconsistent and contradictory in microsystems. Thus, the theoretical approaches become necessary and important.

Now it is commonly recognized that the effects of solid–liquid interface, i.e. the effects of apparent viscosity, boundary slip, EDL, boundary roughness, etc. in microchannel, can be applied to clarify the differences between the experimental results. Lauga and Cossu [18] computed the linear stability of pressure-driven flows with boundary slip in plane microchannel. It was shown that the streamwise sliding delayed the transition significantly, which agrees with the results of Gersting [19] and Min and Kim [20]. You et al. [21] found that the boundary slip always stabilizes the microchannel flow and the apparent viscosity destabilizes the flow. Furthermore, their results indicated the effects of boundary slip are reduced sharply by considering the modification of apparent viscosity. Tardu [22,23] studied the EDL effects on the stability and heat transfer of Poiseuille flow in microchannels. His results showed that the critical Reynolds number decreased considerably when the thickness of the EDL became comparable with the channel diameter. When the effect of EDL is considered, the streaming electrical current balance (ECB) was widely used. However, in the ECB mode, there is an ambiguity point about a reasonless backflow of liquid velocity distribution near the channel wall. To overcome the problem of backflow, a streaming electrical current density balance (ECDB) was proposed recently [24].

As the combined effects of the EDL and boundary slip on microchannel flows are not investigated in previous works, the purpose of this paper is to carry out the investigation on the mean velocity and flow stability by considering the above two effects. Meanwhile, the results of ECDB and ECB modes are compared in detail to get a better understanding on the effects of ECDB on the mean velocity and the stability of microchannel flow.

2. Theory

Liquid flows between two parallel plates with the effects of EDL and boundary slip are considered. The effect of EDL is considered by Poisson–Boltzmann theory and the streaming potential balance mode, where the results of ECB mode and ECDB mode are compared. The effect of boundary slip is considered by Navier slip assumption. The detail of theoretical model is described in the following subsections.

2.1. Electrical double layer

When the characteristic length of flow is decreased to the order of 100 microns, the effect of EDL on flow cannot be ignored. When the solution contains a number of ions, the counterions in the solution are attracted by the electrostatic charges on the solid wall and an electrical field is established. The redistribution of the counterions and ions results in the formation of the EDL near the channel wall. The EDL consisting of compact layer and diffuse layer is shown in Fig. 1. The ions in the compact layer are so strongly attracted by the electrostatic charges on the wall and they are immobile. In diffuse layer, the ions are less attracted to the wall and they are mobile. Consequently, the net charge density across the channel is not zero. The layer boundary is called shear plane. The potential at the shear plane called Zeta potential is measured experimentally.

2.1.1. Poisson–Boltzmann equation

Consider a parallel microchannel separated by a height of $2H$ as shown in Fig. 1. According to the electrokinetics, the relationship of the electrostatic potential ψ and the net charge density ρ_e at certain points in the solution is described by Poisson equation, in y-direction expressed as [22]

$$\frac{\mathrm{d}^2\psi}{\mathrm{d}y^2} = -\frac{\rho_e}{\varepsilon_0\varepsilon} \tag{1}$$

where, ε is the dielectric constant of the solution, ε_0 is the permittivity of vacuum. The net charge density ρ_e is proportional to the concentration difference between positive and negative ions

$$\rho_e = ze(n_+ - n_-) \tag{2}$$

where z is the value of ionic valence, e is the fundamental charge of electron (1.6021×10^{-19} C), n_+ and n_- are the concentration of positive and negative ions, respectively. The ion concentration of EDL electrical field is described by Boltzmann equation as

$$n_\pm = n_0 \exp\left(\mp\frac{ze\psi}{k_bT}\right) \tag{3}$$

where k_b is Boltzmann constant (1.3805×10^{-23} J mol^{-1} K^{-1}), T is the absolute temperature of liquid at the inlet of microchannel (K).

The following dimensionless Poisson–Boltzmann equation is obtained by substituting Eqs. (2), (3) into Eq. (1) and nondimensionalizing the result equation by $\overline{y} = y/H$, $\overline{\psi} = Ze\psi/k_bT$

$$\frac{\mathrm{d}^2\overline{\psi}}{\mathrm{d}\overline{y}^2} = \kappa^2 \sinh(\overline{\psi}) \tag{4}$$

where $\kappa = H \cdot k = H \cdot (2n_0Z^2e^2/k_bT\varepsilon\varepsilon_0)^{1/2}$, k is Debye–Huckel parameter and its inversion $1/k$ is normally referred as the characteristic thickness of the EDL. When the electrical potential is much smaller than the thermal energy of ions ($|Ze\psi| \ll |k_bT|$), Eq. (4) is linearized to

$$\frac{\mathrm{d}^2\overline{\psi}}{\mathrm{d}\overline{y}^2} = \kappa^2\overline{\psi} \tag{5}$$

The dimensionless boundary condition of Eq. (5) is

$$\overline{\psi}(\pm 1) = \overline{\zeta} \tag{6}$$

At the walls, the electrical potential at the interface can be approximated to the potential of shear plane, i.e. $\overline{\psi}_{wall} = \overline{\zeta}$, where $\overline{\zeta} = Ze\zeta/k_bT$. The value of ζ depending on the materials of the system is determined experimentally.

For infinite plane channel flow, the EDL-modified NS equation of pressure-driven flow is [22]

$$\mu\frac{\mathrm{d}^2u}{\mathrm{d}y^2} - \frac{\mathrm{d}p}{\mathrm{d}x} + E_x(y)\rho_e(y) = 0 \tag{7}$$

where the term $E_x(y)\rho_e(y)$ is the electrical force generated by EDL field, μ is the liquid viscosity and $\mathrm{d}p/\mathrm{d}x$ is the pressure gradient. Coupling with the EDL electrical force, the velocity distribution is determined. For a flow driven by hydraulic pressure, the solution ions in diffuse layer are carried down in the streaming direction. The moving net charge results in an electrical current called streaming current I_s. To balance the streaming current, the conduction current I_c is induced in the same magnitude but opposite direction. To determine the conduction current, two modes are available. One is called Electrical Current Balance (ECB) mode [22,23] and the other is Electrical Current Density Balance (ECDB) mode [24].

2.1.2. Mean flow

The effects of EDL and slip boundary on mean flow is studied. As the above discussion, the reasonless backflow of liquid velocity near the channel wall is eliminated by the newly proposed electrical current density balance (ECDB) [24]. In ECDB mode, the equilibrium of the electrical condition in the channel is defined as

$$J_s + J_c = 0 \tag{8}$$

where $J_s = u\rho_e(y)$ and $J_c = \lambda E_x(y)$ are the density of streaming electrical current and conduction current of liquid, respectively. Then the intensity of electrical field is

$$E_x(y) = -u\rho_e(y)/\lambda \tag{9}$$

Substituting this into Eq. (7) yields

$$\mu\frac{\mathrm{d}^2u}{\mathrm{d}y^2} - \frac{\mathrm{d}p}{\mathrm{d}x} - \frac{\rho_e^2(y)}{\lambda}u = 0 \tag{10}$$

By applying $\overline{y} = y/H$, $\overline{u} = u/u_0$, $\overline{\rho}_e = \rho_e/n_0ze$ and the reference velocity $u_0 = -\frac{H^2}{2\mu}\frac{\mathrm{d}p}{\mathrm{d}x}$, the dimensionless form of Eq. (10) is obtained as

$$\frac{\mathrm{d}^2\overline{u}}{\mathrm{d}\overline{y}^2} - 4\frac{G}{\kappa^4}\left(\frac{\mathrm{d}^2\overline{\psi}}{\mathrm{d}\overline{y}^2}\right)^2 \overline{u}(\overline{y}) = -2 \tag{11}$$

where $G = (n_0 zeH)^2/\lambda_0\mu$. The slip boundary condition is considered by Navier assumption

$$u_{wall} = \beta^* \frac{\mathrm{d}u}{\mathrm{d}y}\bigg|_{wall} \tag{12}$$

where β^* is the Navier slip parameter representing the slip length of the flow. In macroscale flows, the no-slip boundary condition is credible because the effect of slip velocity is fairly small. However, in microscale flows, the effect of slip boundary is significant and it should be taken into account. The dimensionless form of the Navier slip boundary condition is

$$\overline{u}(\pm 1) = \mp\beta \frac{\mathrm{d}\overline{u}(\pm 1)}{\mathrm{d}\overline{y}} \tag{13}$$

where $\beta = \beta^*/H$ is the dimensionless Navier slip coefficient.

The mean velocity $\overline{u}(\overline{y})$ is determined by Eq. (11) together with the slip condition (13). The Chebyshev collocation method is used to compute the mean velocity. The details of Chebyshev collocation method are described in Ref. [25].

2.2. Orr–Sommerfeld theory

In the analysis of flow stability under the EDL effect and the slip boundary condition, the classical perturbation theory is used. In this theory, the velocity field is expressed as the sum of mean flow and tiny perturbation, i.e. $u = \overline{u} + u_s$, $v = v_s$ and $p = \overline{p} + p_s$ (the subscript s means perturbation term). By introducing stream function $\Phi(x, y, t) = \phi(y)\exp[i\alpha(x - ct)]$ into the nondimensional continuity and modified NS equations and linearizing the result equation, the O–S equation is obtained as follows:

$$\left[D^2\overline{u} + (i\alpha\mathrm{Re})^{-1}\Delta^2 - (\overline{u} - c)\Delta\right]\phi = 0 \tag{14}$$

where $D = \frac{\mathrm{d}}{\mathrm{d}y}$, $\Delta = D^2 - \alpha^2$, $\mathrm{Re} = u_0 H/\nu$ is the Reynolds number. Here $\overline{u}$ is the mean velocity solution under the combined effect of EDL and slip boundary condition.

The temporal mode is adopted in this study, where the perturbation wave number α is positive real and the perturbation wave speed c is complex. The growth rate αc_i determines the development of perturbation. The corresponding Navier slip boundary is

$$\begin{cases} \phi(\pm 1) = 0 \\ D\phi(\pm 1) = \mp\beta D^2\phi(\pm 1) \end{cases} \tag{15}$$

Eq. (14) together with Eq. (15) controls the flow stability of microchannel flow. The Chebyshev collocation method and QR matrix eigenvalue algorithm are employed to determine the generalized eigenvalue c in Eq. (14).

3. Results and discussion

In this study, two-dimensional microchannel liquid flows are investigated. Assuming the electrical double layer of channel walls is not overlap, Poisson–Boltzmann equation can be applied. First of all, our program is testified by comparing the results of Refs. [18] and [22]. Our results show very good agreement with those of the references.

The combined effects of EDL and boundary slip on microchannel mean flow and stability are the main subject of present approach. The parameter values $\kappa = 41$, $G = 12\,720$ of Ref. [22] are used in this Note.

3.1. Velocity fields

Figure 2 shows the mean velocity profiles of the traditional ECB mode and the newly proposed ECDB mode in the channel and near the channel wall respectively. It shows the maximum velocity in ECDB mode is smaller than that of ECB mode and the effect of EDL apparently restrains the liquid flow rate and results in an inflexion near the channel wall. It is found that there is a reasonless backflow in ECB mode and this backflow is overcome by ECDB mode. Therefore, ECDB mode is adopted in our approach.

Figure 3 shows the velocity distribution in the channel and near the channel wall. The Zeta potential is chosen $\zeta = 2.1254$ as in Ref. [22]. It is found that the effect of EDL apparently restrains the liquid flow rate, which is completely contrary to the effect of boundary slip. For the combined effects of EDL and boundary slip, it is found that the boundary slip is hardly noticed comparing to the pure boundary slip case ($\beta = 0.05$, $\zeta = 0$). This is because the boundary slip velocity $u(\pm 1)$ is proportional to $\frac{\mathrm{d}u(\pm 1)}{\mathrm{d}y}$. The $\frac{\mathrm{d}u(\pm 1)}{\mathrm{d}y}$ value tends to zero due to the strong effect of EDL near the wall. Figure 3b shows the local details of mean flow near wall. It can be seen that the velocity profile of combined effects (open square) is almost

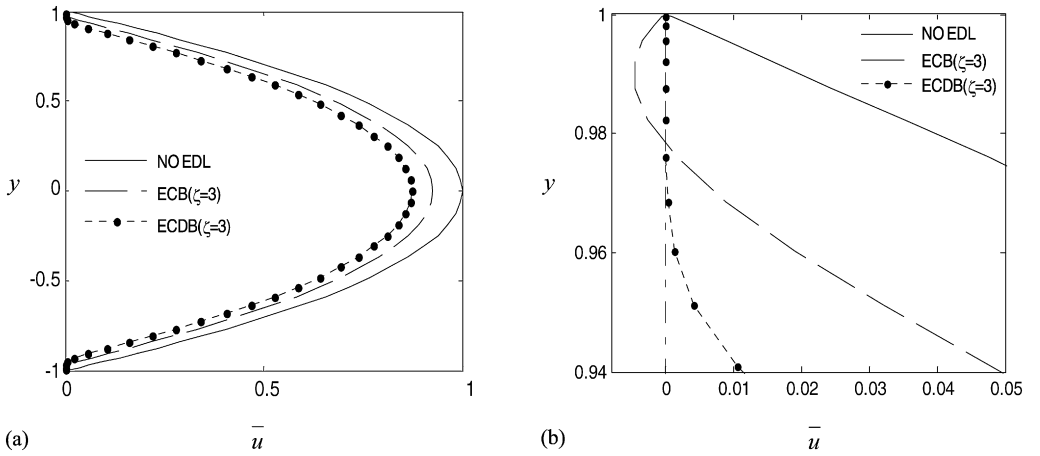

Fig. 2. Comparison of mean velocity distribution of ECB and ECDB mode in microchannel at $\zeta = 3$ and $\beta = 0$, $\kappa = 41$, $G = 12720$. (a) Velocity across the channel; (b) local velocity near the channel wall.

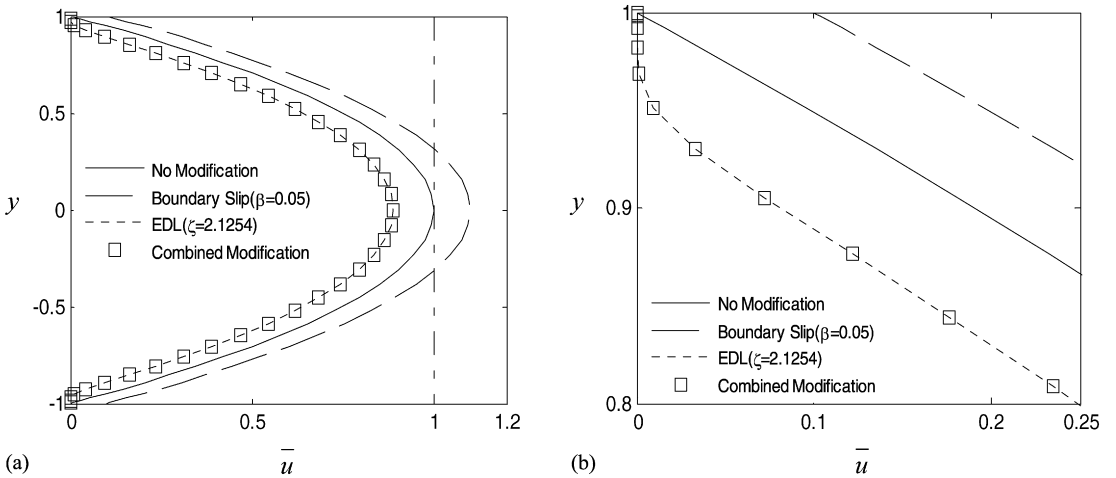

Fig. 3. Mean velocity of ECDB mode at different conditions. (a) Velocity across the channel; (b) local velocity near the channel wall. $\kappa = 41$, $G = 12720$. Solid line $\zeta = 0$, $\beta = 0$ (no modification); long-line dashed $\zeta = 0$, $\beta = 0.05$ (boundary slip); short-line dashed $\zeta = 2.1254$, $\beta = 0$ (EDL effect); hollow square $\zeta = 2.1254$, $\beta = 0.05$ (combined modification).

coincident to that of pure EDL effect. It clearly shows that the effect of boundary slip will be concealed when the Zeta potential is high enough.

Figure 4 shows the velocity distribution in the channel and near the channel wall. In this figure, the Zeta potential is chosen a small number $\zeta = 0.2$. Comparing the result of the combined modification of EDL and boundary slip with that of pure boundary slip, it is found their difference is becoming obvious. Figure 4b shows the local details of mean flow near wall.

Figure 5 shows the velocity profiles corresponding to the effects of EDL, boundary slip and their combined modification for the channel with different material walls. For slip boundary case, as the slip length at each wall is different, the shape of velocity profile is asymmetry. For EDL effect case, the shape of velocity profile is also asymmetry because the high Zeta potential deepens the effect of resistance into the liquid. For the combined modification case, the effect of slip length on the mean velocity at the upper wall is obvious for a small Zeta potential $\zeta = 0.2$ and it is inconspicuous for a large Zeta potential $\zeta = 2$. Generally speaking, the effect of EDL is considerable in microflow systems. It weakens the effect of boundary slip.

3.2. Stability analysis

Figure 6 shows the critical Reynolds number Re_c and the critical wave number α_c with respect to different Zeta potentials and boundary slip length. The crossing point at X-axis is $\alpha_c = 1.02$, $\mathrm{Re}_c = 5772$ corresponding to the no modification case. With the increase of the slip length, the Re_c value increases and the α_c value decreases. It shows that the flow sliding at the wall strengthens the laminar development as well as emphasizes the stability of the flow. The results agree well with

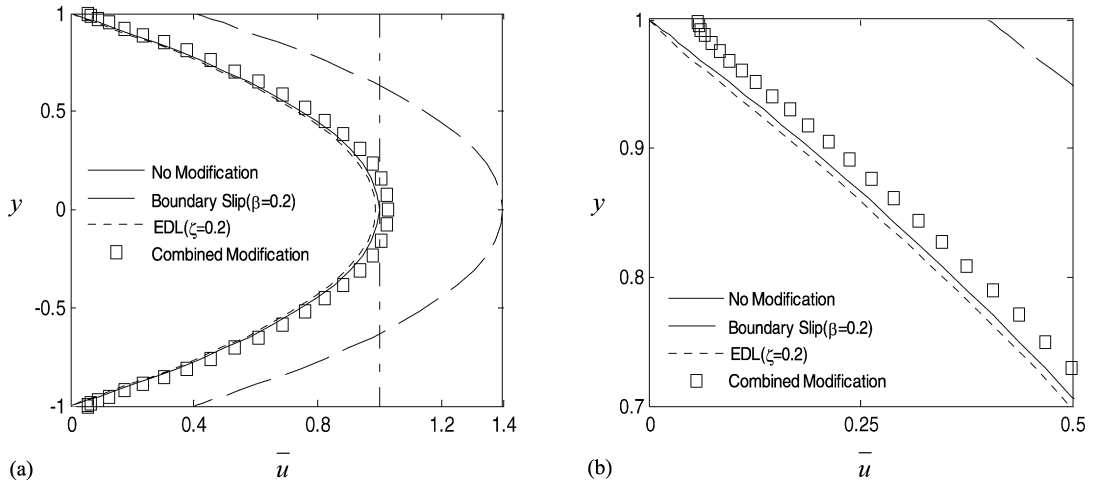

Fig. 4. Mean velocity of ECDB mode at different conditions. $\kappa = 41$, $G = 12\,720$. (a) Velocity across the channel; (b) local velocity near the channel wall. Solid line $\zeta = 0$, $\beta = 0$ (no modification); long-line dashed $\zeta = 0$, $\beta = 0.2$ (pure boundary slip); short-line dashed $\zeta = 0.2$, $\beta = 0$ (EDL effect); hollow square $\zeta = 0.2$, $\beta = 0.05$ (combined modification).

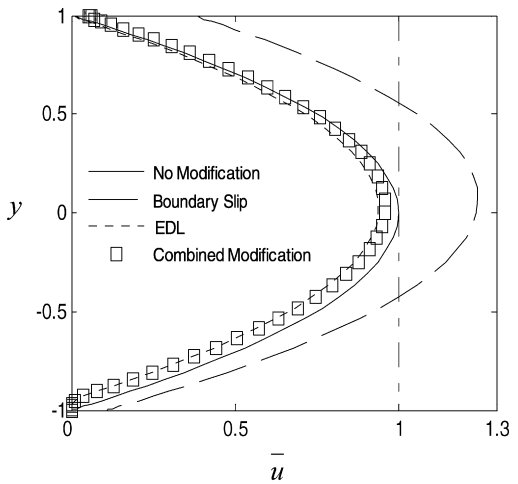

Fig. 5. Mean velocity of ECDB mode at different conditions in a microchannel with different wall materials. $\kappa = 41$, $G = 12\,720$. Solid line $\beta_1 = \beta_2 = 0$, $\zeta_1 = \zeta_2 = 0$ (no modification); long-line dashed $\beta_1 = 0.2$, $\beta_2 = 0.05$, $\zeta_1 = \zeta_2 = 0$ (boundary slip); short-line dashed $\zeta_1 = 0.2$, $\zeta_2 = 2$, $\beta_1 = \beta_2 = 0$ (EDL effects); hollow square $\beta_1 = 0.2$, $\zeta_1 = 0.2$, $\beta_2 = 0.05$, $\zeta_2 = 2$ (combined modification).

those of Lauga and Cossu [18]. On the other hand, with the increase of the Zeta potential, the Re_c value decreases and the α_c value increases. It means the EDL has a destabilizing effect on the microflow. This is because the inflexions on the mean flow caused by EDL lead to an early growth of disturbance.

Figure 7 concerns the combined modification of boundary slip and EDL on the flow stability in the microchannels with the walls of the same and different material. For the same material walls case, the dependence of Re_c on the slip length β with different Zeta potential ζ is illustrated in Fig. 7a. Clearly, when ζ is small ($\zeta = 0.05$), the Re_c value is large and increases strongly with the increase of β, owing to the stabilizing effect of boundary slip. However, when ζ is large enough ($\zeta = 1$), the Re_c begins to decrease slightly with the increase of β. This is because the value of $\frac{\mathrm{d}u(\pm 1)}{\mathrm{d}y}$, i.e. $D^2\phi(\pm 1)$ reduces to zero rapidly with the increase of ζ. Therefore, it means that the boundary slip will have slight effect on the flow stability when ζ is large enough. Figure 7b shows the case of different walls, where the Zeta potential at one wall doubles that at the other wall. The results show that the Re_c decreases with respect to the corresponding case in Fig. 7a for its large Zeta potential at the one wall.

Figure 8 gives a series of neutral curves of combined modification of EDL and boundary slip in microchannels with different wall materials. The results confirm the above conclusions on the combined modification of the EDL and boundary slip. Generally speaking, the effect of boundary slip stabilizes the flow stability; on the contrary, the effect of EDL destabilizes the flow stability. The effectiveness of boundary slip on the flow stability is influenced strongly by the effect of EDL. The effect of boundary slip can be disappeared when the Zeta potential is large enough.

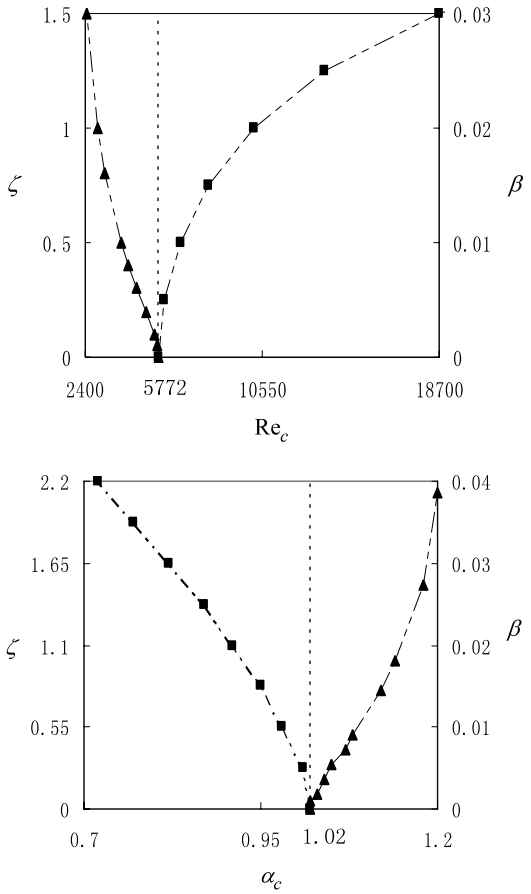

Fig. 6. The critical Reynolds number (Re_c) and critical wave number (α_c) under the effects of EDL and boundary slip, respectively. $\kappa = 41$, $G = 12\,720$. Dashed with solid triangle with respect to the results of EDL effect; dashed with solid square with respect to the results of boundary slip effect.

3.3. Non-modal instability

In the absence of slip at the walls, the Poiseuille flow is known to undergo a transition to turbulence at Reynolds numbers well below the critical Reynolds number corresponding to the onset of linear modal instability ($\mathrm{Re}_c = 5772$). This subcritical transition scenario has been related to the strongly non-normal nature of the linearized O–S operator, explaining the potential of the flow to sustain large transient energy growth, possibly triggering the transition to turbulence at a much lower Reynolds number [26,27]. In this case, the initial perturbations inducing the largest energy growth are streamwise vortices, while the most amplified response consists of streamwise streaks. Lauga and Cossu [18] showed that for the slip boundary case, the shape of the optimal initial perturbation differs slightly from the no-slip case, while the optimal responses are nearly undistinguishable, except near the wall, where the effect of the slip boundary conditions is apparent. The lift-up mechanism, by which low-amplitude vortices are converted into large amplitude streaks, seems therefore to be only slightly sensitive to slip boundary conditions at the wall. It can be concluded that the stabilizing effect of wall-slip is not significant on the non-modal transition in the plane channel flow.

Similar to the wall-slip, it is hopefully anticipated that the shape of the optimal initial perturbation differs slightly from the no-EDL case, while the optimal responses are nearly undistinguishable, except near the wall, where the effect of the EDL boundary conditions is apparent. Therefore, the effect of EDL on the non-modal transition in the plane channel flow is conjectured to be only slightly sensitive to EDL boundary conditions at the wall. It can be further conjectured that the combined effects of wall-slip and EDL on the non-modal transition are not significant in the plane channel flow.

3.4. Application of the theory

The boundary slip depends on many factors, such as hydrophilic or hydrophobic surface, liquid and surface property, etc. In most cases, it is generally recognized that the slip in microchannels is significant only when the height of the channel is of order 1 micron. However, the above conclusion is questionable by the results of experiments in some cases. The boundary slip can be large even when the height of the channel is of order 100 microns or more [28]. In Ref. [18], the micron-resolution particle image velocimetry was applied to measure the velocity profiles of flow through 30×300

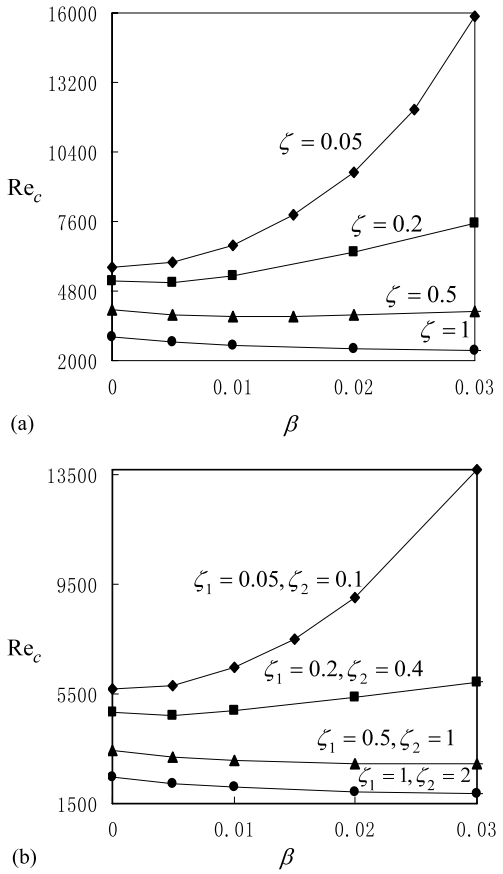

Fig. 7. Critical Reynolds numbers under combined modification of EDL and boundary slip. $\kappa = 41$, $G = 12\,720$. (a) Channel wall with the same material; (b) channel wall with different material.

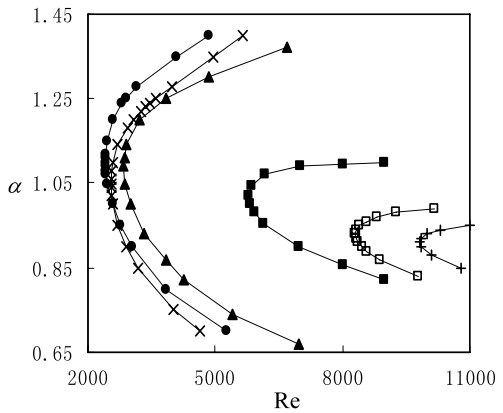

Fig. 8. Neutral curves of combined modification of EDL and boundary slip in different cases. $\kappa = 41$, $G = 12\,720$. Dashed line with different symbol represents the following cases: Solid circle $\zeta_1 = 0.2$, $\zeta_2 = 2$, $\beta_1 = 0.03$, $\beta_2 = 0.01$; multiplication sign $\zeta_1 = 0$, $\zeta_2 = 2$, $\beta_1 = 0.03$, $\beta_2 = 0.01$; solid triangle $\zeta_1 = 0.2$, $\zeta_2 = 2$, $\beta_1 = \beta_2 = 0$; solid square $\zeta_1 = \zeta_2 = 0$, $\beta_1 = \beta_2 = 0$; hollow square $\zeta_1 = 0.2$, $\zeta_2 = 0$, $\beta_1 = 0.03$, $\beta_2 = 0.01$; cross $\zeta_1 = \zeta_2 = 0$, $\beta_1 = 0.03$, $\beta_2 = 0.01$.

micron channel (the height is 30 microns). An apparent slip velocity was found at the wall for water flowing through the microchannel coated with hydrophobic OTS. This slip velocity is approximately 10% of the free-stream velocity and yields a slip length of approximate 1 micron. Feuillebois et al. [29] derived rigorous bounds on the effective slip of two-component textures in thin channels. They concluded that some general principles may hold for thick channels as well.

Although the slippage is observed in many experiments, its mechanism is still under dispute. Most researchers think that there is some gas phase (nanobubbles or a layer of low density of fluid) at the interface between the liquid and the

surface leading to liquid slippage over these surfaces. Moreover, the nanobubble can be detected by many methods. Inspired by these findings, the super-hydrophobic surface covered with micro- or nanostructures was introduced to enhance the slippage of liquid recently because of the entrapped gas in these microstructures. For the super-hydrophobic surface with stripe structure, a slip length of 40 microns for 70 wt% glycerin flow is found in the experiments [30]. By modeling the presence of either a depleted water layer or nanobubbles as an effective air gap at the wall, Tretheway and Meinhart [31] formulated the slip length for flows between two infinite parallel plates as

$$\beta = \frac{1}{2h}\left(\frac{\mu_w}{\mu_a}\right)\left[\delta^2 + 2(\varepsilon + h)\delta + 2\varepsilon h\right]$$

Here, $\varepsilon = \frac{2-\sigma}{\sigma}(\frac{2}{3}\lambda)$. We assume standard conditions for air and water at 20 °C ($\mu_w = 1.0019$ cp, $\mu_a = 0.0183$ cp), a mean free path $\lambda = 100$ nm, an accommodation coefficient $\sigma = 1$ and an air gap thickness $\delta = 20$ nm (the approximate bubble height measured by Tyrell and Attard [32]). For the channel with the height of 100 microns, the slip length is about 4.7 microns. It corresponds to the nondimensional slip length $\beta = 0.094$ in our manuscript.

The stability of microchannel flow is becoming severe only when the channel height is in the order of 100 microns or larger. In the case, the flow Reynolds number can reach the order of 1000, where the results of present approach can be applied.

4. Conclusions

The combined modification of EDL and boundary slip on mean velocity and flow stability are studied for the channel wall made of the same material and different material. By applying the ECDB mode to calculate the flow-induced electrical field, the unreasoned backflow of mean flow in ECB mode near the channel wall is disappeared. The governing equations and boundary conditions can be well solved by Chebyshev collocation method and the eigenvalues can be determined by QR algorithm. The results indicate that the appearance of EDL results in inflexions on the mean velocity profile near channel wall and destabilizes the flow stability. On the contrary, the appearance of boundary slip stabilizes the flow stability. The effectiveness of boundary slip on the mean velocity and flow stability is influenced strongly by the effect of EDL. The effect of boundary slip can be disappeared when the Zeta potential is large enough.

Acknowledgements

The authors wish to acknowledge the support of National Natural Science Foundation of China (20676093).

References

[1] C.M. Ho, Y.C. Tai, Micro-Electro-Mechanical-Systems (MEMS) and fluid flows, Annu. Rev. Fluid Mech. 30 (1998) 579–612.
[2] H.A. Stone, A.D. Stroock, A. Ajdari, Engineering flows in small devices: Microfluidics toward a lab-on-a-chip, Annu. Rev. Fluid Mech. 36 (2004) 381–411.
[3] T.M. Squires, S.R. Quake, Microfluidics: Fluid physics at the nanoliter scale, Rev. Mod. Phys. 77 (2005) 977–1026.
[4] H. Song, J.D. Tice, R.F. Ismagilov, A microfluidic system for controlling reaction networks in time, Angew. Chem. Int. Ed. 42 (7) (2003) 768–772.
[5] B. Zheng, L.S. Roach, R.F. Ismagilov, Screening of protein crystallization conditions on a microfluidic chip using nanoliter-size droplets, J. Am. Chem. Soc. 125 (37) (2003) 11170–11171.
[6] J. Pfahler, J. Harley, H. Bau, et al., Gas and liquid flow in small channels, micromechanical sensors, actuators and systems, in: Winter Meeting of ASME: Micromechanical Sensors, Actuators and Systems, Atlanta, vol. 32, 1991, pp. 49–60.
[7] X.Y. You, X.J. Zheng, J.R. Zheng, Molecular theory of liquid apparent viscosity in microchannels, Acta Phys. Sinica 56 (4) (2007) 2323–2329 (in Chinese).
[8] K. Watanabe, Y. Udagawa, H. Mizunuma, Slip of Newtonian fluids at slid boundary, JSME Int. J. Ser. B 41 (1998) 525–529.
[9] D.C. Tretheway, C.D. Meinhart, Apparent fluid slip at hydrophobic microchannel walls, Phys. Fluids 14 (2002) L9–L12.
[10] C.Y. Soong, S.H. Wang, Theoretical analysis of electrokinetic flow and heat transfer in a microchannel under asymmetric boundary conditions, Journal of Colloid Interface Science 256 (1) (2003) 202–213.
[11] C. Yang, D. Li, Analysis of electrokinetic effects on the liquid flow in rectangular microchannels, Physicochemical and Engineering Aspects 143 (2–3) (1998) 339–353.
[12] X.Y. You, S.H. Li, H.P. Xiao, The effects surface roughness on drag reduction and control of laminar plane microchannel flows, Chemical Engineering (China) 36 (8) (2008) 25–27 (in Chinese).
[13] X.F. Peng, G.P. Peterson, B.X. Wang, Frictional flow characteristics of water flowing through rectangular microchannels, Experimental Heat Transfer 7 (4) (1994) 249–264.
[14] B. Xu, et al., Experimental investigation of flow friction for liquid flow in microchannels, International Communications in Heat and Mass Transfer 27 (8) (2000) 1165–1176.
[15] J. Judy, D. Maynes, B.W. Webb, Characterization of frictional pressure drop for liquid flows through microchannels, International Journal of Heat and Mass Transfer 45 (17) (2002) 3477–3489.
[16] K.V. Sharp, R.J. Adrian, Transition from laminar to turbulent flow in liquid filled microtube, Experiments in Fluids 36 (5) (2004) 741–747.
[17] P.F. Hao, F. He, K.Q. Zhu, Flow characteristics in a trapezoidal silicon microchannel, Journal of Micromechanics and Microengineering 15 (6) (2005) 1362–1368.
[18] E. Lauga, C. Cossu, A note on the stability of slip channel flows, Physics of Fluids 17 (2005) 088106.
[19] J.M. Gersting, Hydrodynamic stability of plane porous slip flow, Physics of Fluids 17 (11) (1974) 2126–2127.
[20] T. Min, J. Kim, Effects of hydrophobic surface on stability and transition, Physics of Fluids 17 (2005) 108106.
[21] X.Y. You, J.R. Zheng, Q. Jing, Effects of boundary slip and apparent viscosity on the stability of microchannel flow, Forschung im Ingenieurwesen 71 (2007) 99–106.
[22] S. Tardu, The electric double layer effect on the microchannel flow stability and heat transfer, Superlattices and Microstructures 35 (2004) 513–529.

[23] S. Tardu, Interfacial electrokinetic effect on the microchannel flow linear stability, Journal of Fluids Engineering – Transactions of the ASME 126 (1) (2004) 10–13.
[24] L. Gong, J.K. Wu, Resistance effect of electric double layer on liquid flow in microchannel, Applied Mathematics and Mechanics 27 (10) (2006) 1391–1398.
[25] X.Y. You, Feedback control of the instability of a fluid layer flowing down a vertical cylinder, International Journal of Heat and Mass Transfer 45 (22) (2002) 4537–4542.
[26] L.N. Trefethen, A.E. Trefethen, S.C. Reddy, T.A. Driscoll, Hydrodynamic stability without eigenvalues, Science 261 (1993) 578–582.
[27] P.J. Schmid, D.S. Henningson, Stability and Transition in Shear Flows, Springer, New York, 2001.
[28] K. Watanabe, Y. Udagawa, H. Udagawa, Drag reduction of Newtonian fluid in a circular pipe with a highly water-repellent wall, J. Fluid Mech. 381 (1999) 225–238.
[29] F. Feuillebois, M.Z. Bazant, O.I. Vinogradova, Effective slip over superhydrophobic surfaces in thin channels, Phys. Rev. Lett. 102 (2009) 026001.
[30] J. Li, et al., On the measurement of slip length for liquid flow over super-hydrophobic surface, Chinese Science Bulletin 54 (24) (2009) 4560–4565.
[31] D.C. Tretheway, C.D. Meinhart, A generating mechanism for apparent fluid slip in hydrophobic microchannels, Phys. Fluids 16 (5) (2004) 1509–1515.
[32] J. Tyrell, P. Attard, Images of nanobubbles on hydrophobic surfaces and their interactions, Phys. Rev. Lett. 87 (2001) 176104.